

Experimental Observations of Laser-Driven Tin Ejecta Microjet Interactions

A. M. Saunders,¹ C. V. Stan,¹ K. K. Mackay,¹ B. Morgan,¹ J. A. K. Horwitz,¹ S. J. Ali,¹ H. G. Rinderknecht,² T. Haxhimali,¹ Y. Ping,¹ F. Najjar,¹ J. Eggert,¹ and H.-S. Park¹

¹Lawrence Livermore National Laboratory

²Laboratory for Laser Energetics, University of Rochester

The study of metal ejecta microjet interactions has broad applicability to fields ranging from planetary formation¹ to cloud interaction dynamics.² An ejecta microjet forms when a strong shock travels through a metal sample and, upon reaching the opposite side, interacts with a micron-scale surface perturbation, such as a dent or a groove. The surface perturbation then inverts to form a jet of micron-scale material traveling at a high velocity, often exceeding 1 km/s (~ 2200 mi/h) (Ref. 3). The jet is comprised of particles with average diameters of ~ 1 μm (Ref. 4). While extensive work has been performed to understand microjet formation and evolution, collisions of interacting microjets have been neglected. We present the first measurements of interaction behavior between two high-velocity tin ejecta microjets as captured through sequences of x-ray radiography images from experiments on the OMEGA EP laser.

Figure 1(a) shows a schematic of the ejecta platform. The targets consist of two tin foils with an angle of 130° between target normals. The foils have grooves carved into their interior surfaces, which traverse the entire foils and are 45 μm deep with 60° opening angles. Figure 1(b) shows a photo of the assembled targets. The tin foils are 100 μm thick with 30 - μm -thick plastic ablaters on their front surfaces to increase laser drive efficiency. They are irradiated with two 8-ns square laser pulses with tunable energy, driving shock waves into the tin. Figure 1(c) shows pressure profiles from radiation-hydrodynamic simulations performed using Ares⁵ at three different times for the sample case of a 11.7-GPa shock. After a delay, a 500-J, 100-ps short-pulse laser heats a 20- μm titanium microwire as a bright x-ray point source to image along the axis perpendicular to the flow of both planar microjets with a resolution of 20 μm . Figures 1(d) and 1(e) show analyzed radiographs of interacting jets from targets with laser drives of 70 J and 1200 J, producing shock pressures of 11.7 GPa and 116 GPa, respectively. We observe densities up to 30 and 150 mg/cm^3 for the two cases. The density relates linearly to the packing density (or “volume fraction”) of particles within the jetting material. From our analysis, the volume fractions in the microjets reach up to 0.3% for the lower-pressure drive and 1.5% for the higher-pressure drive. Analysis of the lower-pressure jets shows that the jets pass through each other unattenuated, maintaining the same velocity and density distributions. In comparison, the higher-pressure jets generate a cloud of material upon interaction, suggesting a higher probability of particle collisions.

Simulations of the jetting tin identified three different regimes: a low-energy regime where material strength inhibits jet formation, a moderate-energy regime where the tin is a mixed solid–liquid material, and a high-energy regime where the tin is expected to be fully melted.⁶ The 11.7-GPa and 116-GPa cases are in the moderate- and high-energy regimes, respectively. Simulations of two interacting microjets for a 11.7-GPa shock exhibit the same unattenuated behavior that is observed in the experiments. Figure 2 shows simulated jet interactions from 116-GPa shocks. We characterize the spread of the interaction cloud for both the simulations and the data in the R - and the S -directions indicated in Fig. 2(a). The spread along R [Fig. 2(b)] corresponds with the extent of the cloud from the center of the interaction point in the direction of jet propagation and assesses how much the jet slows in its original direction of propagation. The spread in the S direction [Fig. 2(c)] quantifies the vertical extent of the projection onto the center axis of symmetry. Both are defined as the widths between a volume fraction cutoff of 0.1%. The hypothetical linear extents for unattenuated jets are depicted with dashed orange lines. The simulation captures the observed slowing from

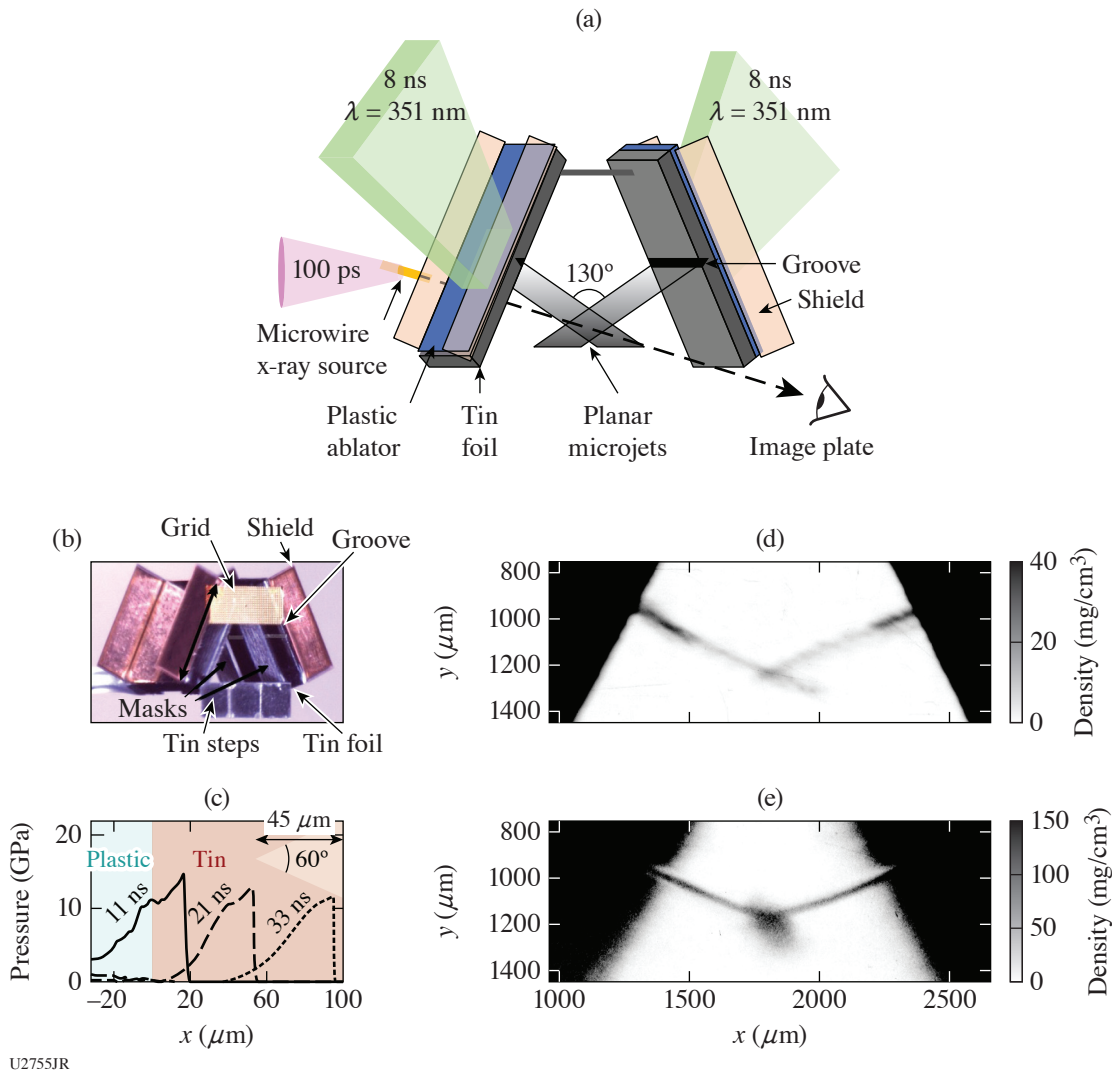


Figure 1

(a) Schematic of the tin microjet interaction platform. Two long-pulse lasers drive shocks into tin foils with grooves carved into their rear surfaces. A short-pulse laser on a microwire generates x rays for radiography. (b) Photo of the target indicating key elements and dimensions. Tin steps of known thicknesses are used for density calibration in radiographs. Masks limit the jet region that propagates to the interaction point. (c) Simulated spatial variations of pressure at three times. Groove schematic is overlaid on simulation results. [(d),(e)] Two analyzed radiographs from drive pressures of 11.7 and 116.0 GPa, respectively. The higher-pressure drive results in densities that are 5× higher than the lower-pressure case.

6.5 km/s to 4.5 km/s after interaction in Fig. 2(b); the collisions between particles result in altered mass-velocity distributions of the particles such that the particles travel in many directions, generating a cloud. Figure 2(c), however, shows that the observed vertical extent of the cloud exceeds the predicted value. Lineouts of the spread in both the R and S directions for the data and simulations show similar qualitative characteristics, with higher-density regions at the center of interaction followed by densities tapering with increased distance from the center. However, the simulations show up-to 30% higher density at the center point of interaction, again suggesting that the simulations do not capture the full spread behavior.

More experiments are needed to understand both the collision model deficiencies and the onset of interaction behavior as a function of shock pressure, but these experiments provide the first data on interacting ejecta microjet behavior and a novel methodology to observe the interactions of high-velocity, particle-laden flows, which opens many more avenues for detailed study.

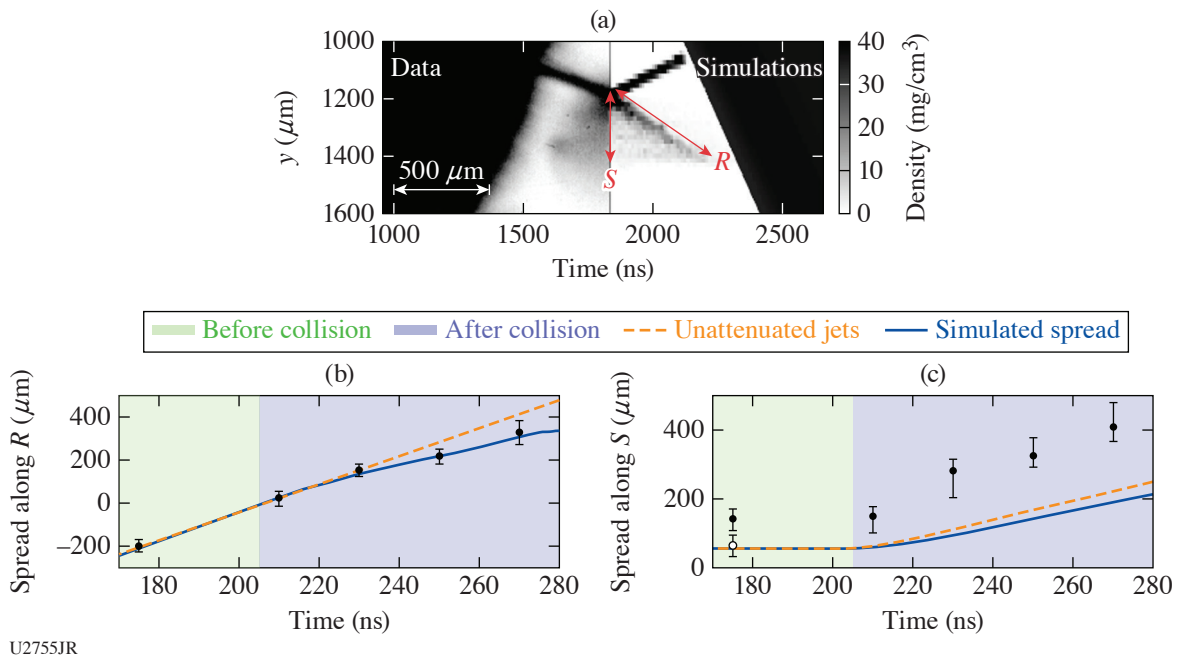


Figure 2

High-pressure shock data and simulations for particle spread. (a) Density maps for the data (left) and simulations (right). Spread as measured along the R and S directions is indicated. (b) The spread of the microjet cloud in the direction of jet propagation as measured from the center point of the interaction (R direction): simulations (blue line), experiments (black points). (c) The projection of jet extent onto the axis of symmetry (S direction). The points before collision indicate the vertical extent of a single jet: the bulk of the jet (white) and the small bulbous region near the front of the jet (black). The orange lines indicate the hypothetical linear extent of unattenuated jets.

This material is based upon work supported by the Department of Energy National Nuclear Security Administration under Award Number DE-NA0003856, the University of Rochester, and the New York State Energy Research and Development Authority.

1. M. Lambrechts and A. Johansen, *Astron. Astrophys.* **544**, A32 (2012).
2. Z. Warhaft, *Fluid Dyn. Res.* **41**, 011201 (2008).
3. K. O. Mikaelian, *Phys. Rev. Lett.* **80**, 508 (1998).
4. D. S. Sorenson *et al.*, *J. Appl. Phys.* **92**, 5830 (2002).
5. R. M. Darlington, T. L. McAbee, and G. Rodrigue, *Comp. Phys. Commun.* **135**, 58 (2001).
6. K. K. Mackay *et al.*, *J. Appl. Phys.* **128**, 215904 (2020).